

RESEARCH

Open Access



A mouse model of ATRX deficiency with cognitive deficits and autistic traits

Katherine M. Quesnel^{1,2,3}, Nicole Martin-Kenny^{1,2,3} and Nathalie G. Bérubé^{1,2,3,4*} 

Abstract

Background ATRX is an ATP-dependent chromatin remodeling protein with essential roles in safeguarding genome integrity and modulating gene expression. Deficiencies in this protein cause ATR-X syndrome, a condition characterized by intellectual disability and an array of developmental abnormalities, including features of autism. Previous studies demonstrated that deleting ATRX in mouse forebrain excitatory neurons postnatally resulted in male-specific memory deficits, but no apparent autistic-like behaviours.

Methods We generated mice with an earlier embryonic deletion of ATRX in forebrain excitatory neurons and characterized their behaviour using a series of memory and autistic-related paradigms.

Results We found that mutant mice displayed a broader spectrum of impairments, including fear memory, decreased anxiety-like behaviour, hyperactivity, as well as self-injurious and repetitive grooming. Sex-specific alterations were also observed, including male-specific aggression, sensory gating impairments, and decreased social memory.

Conclusions Collectively, the findings indicate that early developmental abnormalities arising from ATRX deficiency in forebrain excitatory neurons contribute to the presentation of fear memory deficits as well as autistic-like behaviours.

Keywords Intellectual disability, Autism, ATRX, Sex differences, Mice

Introduction

Intellectual disability (ID), defined as early onset deficits in cognitive function that lead to difficulties in daily tasks and social skills [1], impacts 1-2% of school aged children [2] and poses both social and medical challenges. Autism spectrum disorder (ASD) is another neurodevelopmental condition with high prevalence (1-2%)

and is characterized as social communication difficulties with the presence of stereotyped or repetitive behaviours [3–5]. Many patients with neurodevelopment disorders have co-occurring conditions and often disorders overlap in their defining characteristics. Clinical studies suggest that ~70% patients with ASD display a form of learning or intellectual disability. Additionally, anxiety and hyperactivity are associated features of ASD and 68% of patients with ASD have been reported to display aggression at some point [3, 6, 7]. These overlapping features in neurodevelopmental disorders suggest that similar molecular pathways and neural circuitry are disrupted across disorders.

Chromatin structure modulation and epigenetic mechanisms have been implicated in cognitive processes and many genes mutated in ID and ASD encode chromatin regulatory factors [8–10]. Many of these chromatin

*Correspondence:
Nathalie G. Bérubé
nberube@uwo.ca

¹ Department of Anatomy & Cell Biology, Western University, London, Canada

² Department of Paediatrics, Western University, London, Canada

³ Division of Genetics & Development, Children's Health Research Institute, London, ON, Canada

⁴ Department of Oncology, Western University, London, Canada



remodelers are known to interact with one another in processes important for neurodevelopment and plasticity [11]. Alpha thalassemia mental retardation, X-linked (ATR-X) is an ATP-dependent chromatin remodeling protein that maintains chromatin structure integrity and regulates gene expression. Hypomorphic mutations in the *ATR-X* gene result in ATR-X syndrome, a congenital syndrome that primarily affects males, as females are protected by skewed X-chromosome inactivation [12]. Patients with ATR-X syndrome show a variety of symptoms including mild-to-severe intellectual disability, seizures, microcephaly, and dysmyelination.

In addition to intellectual disability, a subset of ATR-X syndrome patients also display autistic features [13–15]. Moreover, *ATR-X* mutations have been observed in non-syndromic patients with ID [16] and have been identified in patients with ASD [17, 18]. The SFARI gene database ranks *ATR-X* as a Category 1 (High Confidence) risk gene implicated in ASD (<https://gene.sfari.org/>). Based on these reports we can confidently infer that mutations in *ATR-X* are highly associated with both ID and ASD.

ATR-X is localized at heterochromatic regions of the genome and is involved in maintaining repressive states required for genomic integrity [19–22]. The role of *ATR-X* in preserving genomic integrity is crucial in actively dividing cells. Conventional knockout mice cannot be generated since *ATR-X*-null embryonic stem cells are too unstable. Deletion of *ATR-X* in early stages of embryogenesis or in neuronal progenitor cells results in embryonic or early post-natal death [23–25]. Further investigation indicated an increase in DNA damage and TP53-induced cell death upon loss of *Atrx* in neural progenitor cells [24–26]. Therefore, to study how *ATR-X* dysfunction leads to the clinical phenotypes observed, conditional inactivation approaches were applied to inactivate *ATR-X* specifically in non-proliferating (post-mitotic) cells to avoid DNA replication stress-mediated cell death. We previously reported that deletion of *ATR-X* in excitatory forebrain neurons using the α CaMKII-Cre line of mice led to male-specific deficits in long-term hippocampal-dependent spatial memory and transcriptional changes relating to synaptic regulation [27]. However, autistic phenotypes were not present in either male or female *Atrx*^{CaMKII-Cre} mice [28].

This led us to hypothesize that perhaps an earlier deletion of *Atrx* might be required to replicate clinically observed cognitive deficits and features of ASD. In the current study, we utilized the NEX-Cre driver line of mice to delete *Atrx* in postmitotic neurons of the embryonic forebrain beginning at E11.5 [29]. These animals survive to adulthood, allowing thorough assessment of their behaviour. A battery of tests revealed that *Atrx*^{NEX-Cre} male and female mice have impaired fear memory as

well as ASD features. We also observed sexually dimorphic behaviour differences, including male-specific aggressivity and altered sensory gating. Overall, these mice represent a clinically relevant model to study the underlying causes of ASD and ID caused by *ATR-X* deficiency in neurons.

Results

Generating mice with *ATR-X* deletion in excitatory neurons of the embryonic forebrain

Mice were generated that lack *Atrx* in forebrain post-mitotic excitatory neurons starting at embryonic day (E)11.5, using the NEX-Cre driver line of mice [29]. Neuronal helix-loop-helix protein-1 (NEX, also called NeuroD6) is a transcription factor expressed in post-mitotic immature neurons of the dorsal forebrain and is involved in terminal differentiation [30]. We confirmed loss of *ATR-X* by immunohistochemistry of coronal brain cryosections at E13.5 and P20. The results show that by E13.5, loss of *ATR-X* is apparent in the cortical plate where neurons begin differentiation and express β III-tubulin (Fig. 1A, B). At P20, *ATR-X* staining demonstrates that the protein is absent in NeuN-positive neurons of *Atrx*^{NEX-Cre} male cortex and hippocampus (Fig. 1C, D). We note that *ATR-X* protein is still expressed in a subset of cells in the dentate gyrus of the hippocampus at P20 and 3 months, likely corresponding to neuroprogenitor cells and GABAergic interneurons [31]. *ATR-X* deficiency was also confirmed in *Atrx*^{NEX-Cre} female brain cryosections at E13.5 and P20 (Fig. S1 A-D).

Memory impairments in *Atrx*^{NEX-Cre} mice

Learning and memory paradigms are used in animal models to measure cognitive deficits that compare to intellectual disabilities clinically. Two common learning and memory paradigms used to evaluate mouse models of ID are the fear memory test and the Morris water maze paradigm [32, 33]. First, we utilized the fear memory test, where mice are placed in an opaque box with distinct visual patterns on the side and a metal grate flooring for 3 minutes during the conditioning portion of the test. At the 2.5-minute mark, animals receive a foot-shock through the metal grate floor. We observed that all mice regardless of sex or genotype had an equivalent initial freezing response to the shock (Fig. 2A). In the memory portion of the test, animals are placed back in the same apparatus either 1.5 or 24 hours post foot-shock, and freezing behaviour is measured. We found that male and female *Atrx*^{NEX-Cre} mice spend significantly less time freezing compared to sex-matched control mice at 1.5 hours (Male: $p < 0.0001$, $F = 1.299$; Female: $p < 0.0001$, $F = 3.250$) and 24 hours post foot shock (Male: $p = 0.0002$, $F = 2.019$; Female: $p < 0.0001$, $F = 2.830$) (Fig. 2B,

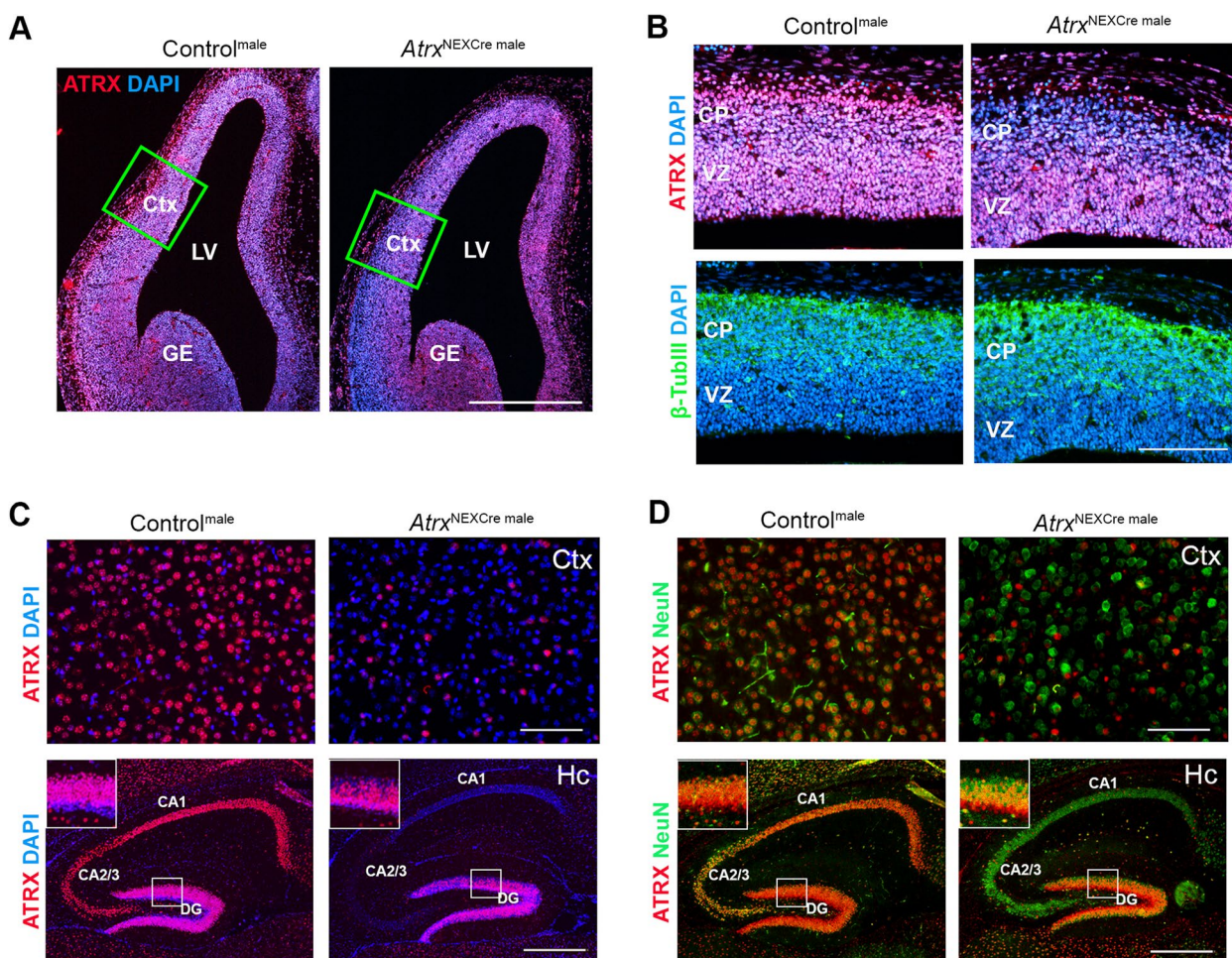


Fig. 1 Validation of *Atrx* deletion in *Atrx*^{NEXCre} male mice. **A** ATRX immunofluorescence staining of E13.5 control and *Atrx*^{NEXCre} brain coronal cryosections is shown in red. DAPI counterstaining is shown in blue. Scale bar, 570 μ m. **B** Magnified view of ATRX (top, red) and β III-tubulin (bottom, green) staining in the developing cortical plate. Scale bar, 144 μ m. **C** ATRX (red) and DAPI (blue) staining in the cortex and hippocampus of *Atrx*^{NEXCre} and control mice at P20. **D** ATRX (red) and NeuN (green) staining in the cortex and hippocampus at P20. Cortex scale bar, 100 μ m and hippocampus scale bar, 400 μ m. CA: cornu Ammonis, CP: cortical plate, Ctx: cortex, DG: dentate gyrus, GE: ganglionic eminence, LV: lateral ventricle, VZ: ventricular zone

C), suggesting that loss of ATRX causes deficits in fear memory.

For the Morris water maze, mice are placed into a water bath and trained with 4 trials per day for 4 days to find a submerged platform using spatial cues [33]. When mice were unable to find the platform during the 90 second trial, they were guided to the platform and a time of 90 seconds was reported for the trial. Male and female *Atrx*^{NEXCre} mice failed to find the platform, over the 4 days of training (Fig. S2A). We also observed that during the training phase, the *Atrx*^{NEXCre} mice gradually spend less time swimming, remain close to the wall, or display floating behaviour (Fig. S2B, Movie 1). Since the *Atrx*^{NEXCre} mice were

not able to learn the task, we were unable to test spatial memory using this paradigm. To explore whether failure in the learning phase of the Morris water maze could be caused in part by increased apathy, we performed a 6-minute forced swim test, where animals are placed in a tall cylinder of water for 6-minutes and time immobile is measured [34]. The results show that *Atrx*^{NEXCre} male mice spend more time immobile compared to sex-matched controls ($p=0.0292$, $F=2.028$) suggesting that they experience apathy in water (Fig. S2C). Conversely, female *Atrx*^{NEXCre} mice spend less time immobile ($p=0.0154$, $F=3.149$). Calculation of the sex discrimination index reveals a significant sex difference in apathetic behaviour in response to water ($p=0.0002$, $F=2.370$).

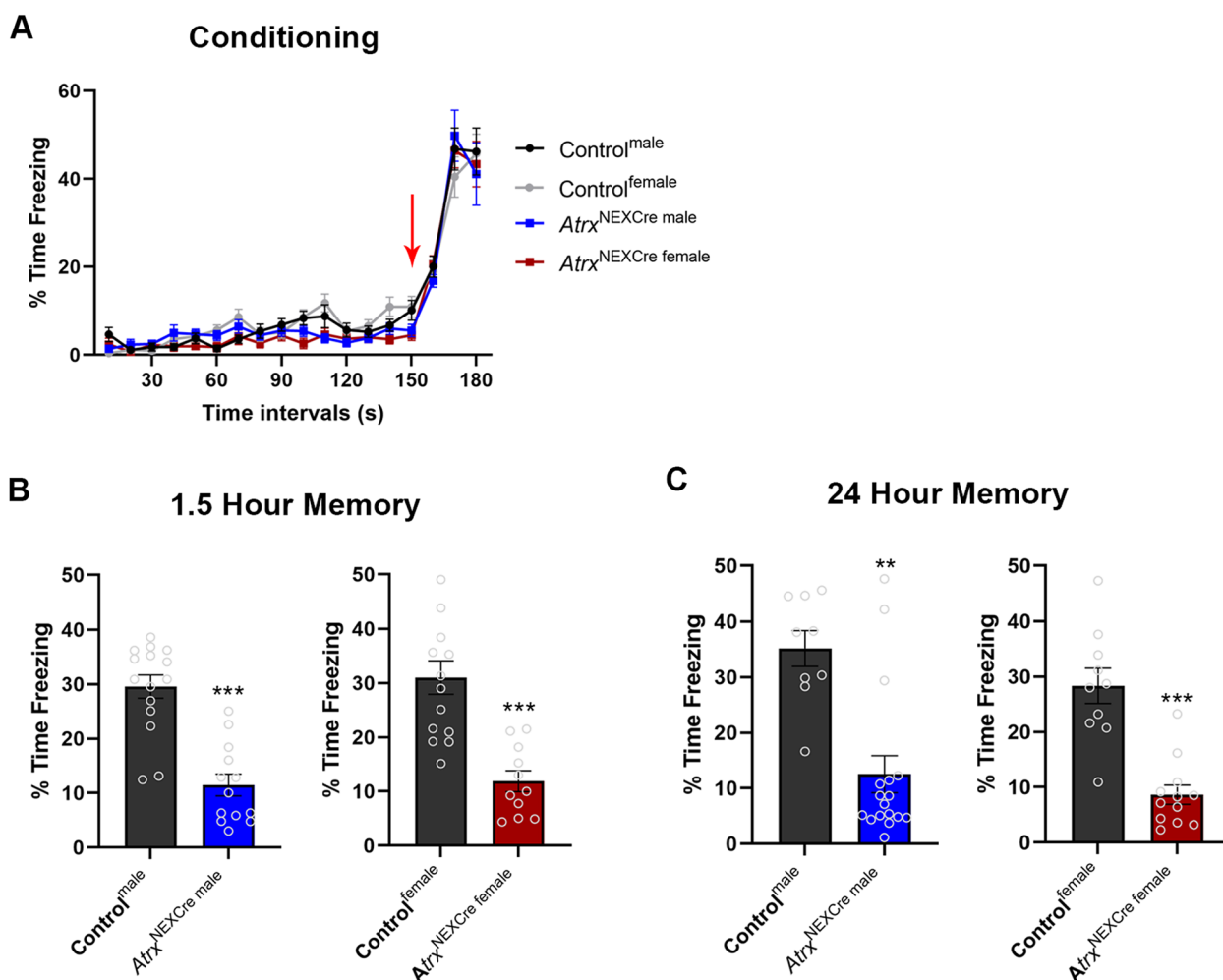


Fig. 2 Fear memory deficits in male and female *Atrx^{NEXCre}* mice. **A** 3-month-old mice were placed in fear apparatus for 3-minutes and received a foot-shock at 2.5-minutes (red arrow). Mice of each sex and genotype as indicated responded with increased freezing after the foot-shock. **B, C** *Atrx^{NEXCre}* mice spent significantly less time freezing compared to control mice at 1.5 and 24 hours after foot shock (1.5 hours male: $p < 0.0001$, $F = 1.299$, Control^{male} $n = 15$, *Atrx^{NEXCre}* male $n = 13$. 1.5 hours female: $p < 0.0001$, $F = 3.240$, Control^{female} $n = 14$, *Atrx^{NEXCre}* female $n = 11$. 24 hours male: $p = 0.0002$, $F = 2.019$, Control^{male} $n = 9$, *Atrx^{NEXCre}* male $n = 17$. 24 hours female: $p < 0.0001$, $F = 2.830$, Control^{female} $n = 10$, *Atrx^{NEXCre}* female $n = 12$). Error bars represent \pm SEM (Students t-test, ** $p < 0.001$, *** $p < 0.0001$)

Hyperactivity, decreased anxiety-like behaviour and repetitive grooming in *Atrx^{NEXCre}* mice

Hyperactivity disorders are often co-diagnosed in ASD patients and ASD mouse models [35, 36]. We therefore tested activity levels and observed that male and female *Atrx^{NEXCre}* mice display hyperactivity as measured by distance travelled and velocity in an open field (Male: Distance $p < 0.0001$, $F = 6.974$, Velocity $p = 0.0009$, $F = 3.678$; Female: Distance $p < 0.0001$, $F = 13.02$, Velocity $p = 0.0012$, $F = 4.256$) (Fig. 3A, B).

Time spent in the center of the open field is used as a measure of anxiety-like behaviour in rodent models. There was no difference in the time spent in the center between control and *Atrx^{NEXCre}* mice (Fig. 3C). Since

the *Atrx^{NEXCre}* mice are hyperactive, we also tested the distance travelled in the center. *Atrx^{NEXCre}* male and female mice travelled significantly more distance in the center of the open field compared to sex-matched controls (Male: $p < 0.0001$, $F = 2.691$, Female: $p = 0.0012$, $F = 4.256$) suggesting that loss of neuronal ATRX may have anxiolytic effects (Fig. 3D). However, the increased locomotor activity could also be a confounding variable when examining the distance travelled in center. Therefore, to further support these findings, *Atrx^{NEXCre}* mice were evaluated in the light-dark box paradigm for 15-minutes, and the amount of time spent in the open and light area compared to the enclosed dark space was measured. Both male and female *Atrx^{NEXCre}* mice spent

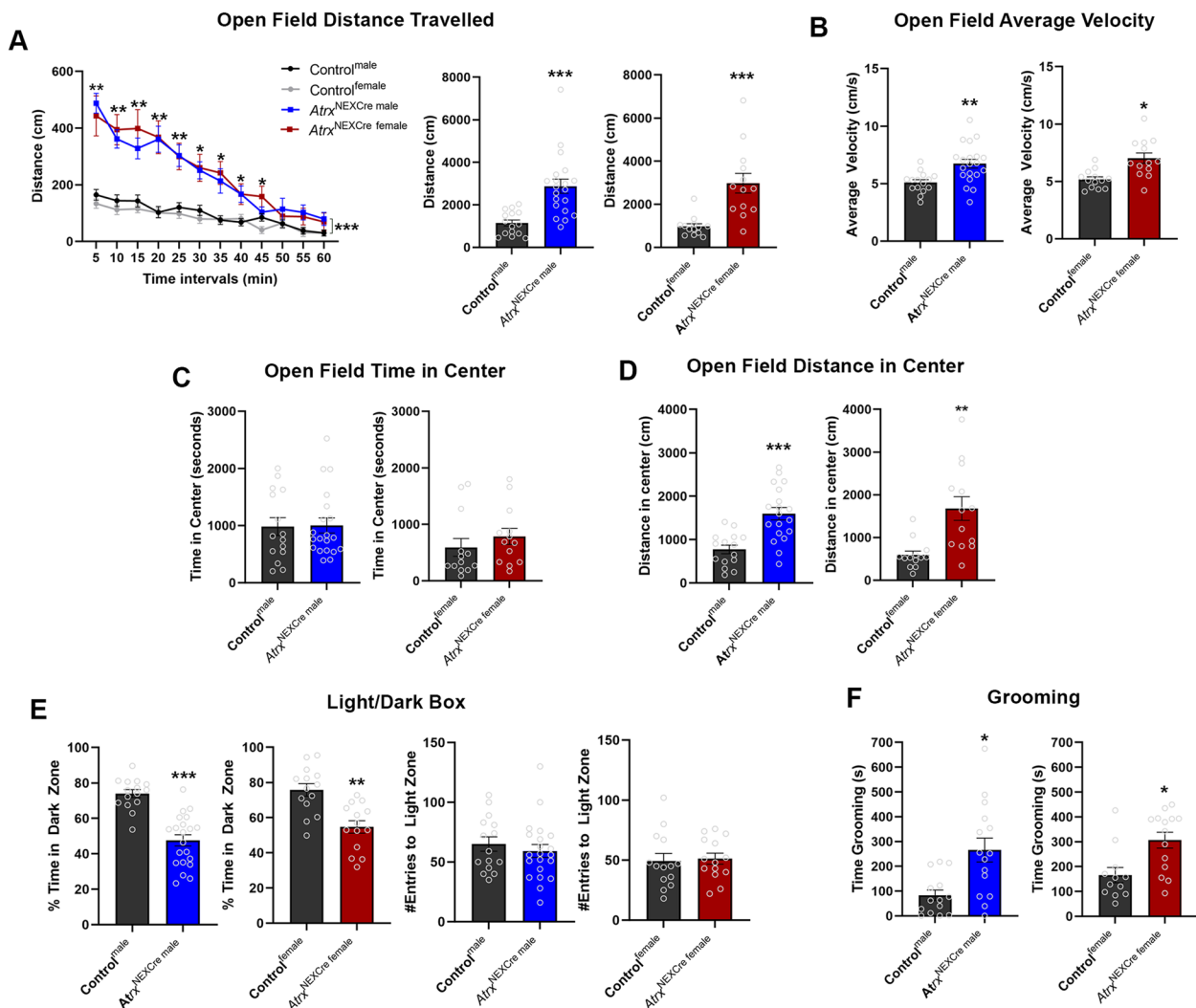


Fig. 3 *Atrx*^{NEXCre} mice are hyperactive, show reduced anxiety-like behaviour, and overgroom compared to control mice. **A** Open field testing of *Atrx*^{NEXCre} male and female mice shows significantly increased locomotor movement compared to controls as seen over-time in 5-minute intervals and total distance travelled in 1 hour (Male: $p < 0.0001$, $F = 6.974$, Control^{male} $n = 15$, *Atrx*^{NEXCre male} $n = 20$; Female: $p < 0.0001$, $F = 13.02$, Control^{female} $n = 13$, *Atrx*^{NEXCre female} $n = 13$). **B** Loss of ATRX in excitatory neurons results in significantly increased velocity of movement (Male $p = 0.0009$, $F = 3.678$, Female $p = 0.0012$, $F = 4.256$). **C** No alterations in the time spent in the center of the open field was detected, however there was a **D** decreased distance travelled in the center of the open-field (Male $p < 0.0001$, $F = 2.691$, Female $p = 0.0004$, $F = 9.146$). **E** Time spent in the dark zone in the light-dark box paradigm (Male: $p < 0.0001$, $F = 2.746$, Control^{male} $n = 15$, *Atrx*^{NEXCre male} $n = 21$, Female: $p = 0.0003$, $F = 1.016$, Control^{female} $n = 14$, *Atrx*^{NEXCre female} $n = 14$) and the number of entries into the light zone. **F** Adult *Atrx*^{NEXCre} mice spend more time grooming than control mice (Male: $p = 0.0030$, $F = 5.450$, Control^{male} $n = 18$, *Atrx*^{NEXCre male} $n = 15$, Female: $p = 0.0042$, $F = 1.016$, Control^{female} $n = 12$, *Atrx*^{NEXCre female} $n = 14$). Error bars represent +/-SEM. Students t-test, Mann Whitney, or Two-way Anova with Sidak post-hoc (* $p < 0.05$, ** $p < 0.001$, *** $p < 0.0001$)

significantly less time in the dark area compared to controls (Male: $p < 0.0001$, $F = 2.746$, Female: $p = 0.0003$, $F = 1.016$). The number of entries from the dark into the light compartment and vice versa was not significantly different between *Atrx*^{NEXCre} and control mice, indicating that higher activity levels exhibited by mutant mice cannot account for the increased time spent in the light. (Fig. 3E). We also attempted to evaluate anxiety-related behaviour in the elevated plus maze, however

the *Atrx*^{NEXCre} mice jumped off the apparatus and could not complete the task.

Repetitive behaviours represent a core autistic feature that is apparent by an overgrooming phenotype in mice [4], and was evaluated in control and *Atrx*^{NEXCre} mice over a 15-minute period. This revealed that male and female *Atrx*^{NEXCre} mice display repetitive behaviours, as shown by increased time spent grooming (Male: $p = 0.0030$, $F = 5.450$, Female: $p = 0.0042$, $F = 1.281$) (Fig. 3F).

Repetitive grooming in some mice led to large patches of fur missing, and in severe cases, mice needed to be euthanized for self-injuries (Fig. S3A).

Sensory gating and olfactory deficits in *Atrx*^{NEXCre} mice

Sensory processing abnormalities are implicated in patients with ASD. To test this phenotype, we utilized a pre-pulse inhibition test to examine startle response and sensory gating [28, 37]. First, animals were exposed to 50 trials of a 115 db pulse, lasting 20 ms with 20 s between each trial. We observed an exaggerated startle response to this acoustic stimulus in male, but not female *Atrx*^{NEXCre} mice (Male: $p=0.0008$, $F=18.08$)

(Fig. 4A). Next, animals were exposed to the pre-pulse inhibition portion of the test, consisting of a pulse only at 115 db, 40 ms in length, and four types of pre-pulse trials: Type 1: 75 db, 30 ms prior to the startle pulse, Type 2: 80 db, 30 ms prior to startle, Type 3: 75 db, 100 ms prior to startle, and Type 4: 80 db, 100 ms prior to startle. Male *Atrx*^{NEXCre} mice displayed decreased pre-pulse inhibition compared to controls (Male: Type 1: $p=0.0286$, $F=1.414$, Type 2: $p=0.0261$, $F=2.048$, Type 3: $p=0.0042$, $F=1.549$, Type 4: $p=0.0008$, $F=2.510$). Conversely, female *Atrx*^{NEXCre} mice did not show a similar reduction in PPI (Fig. 4B, C). Statistical analysis reveals a significant sex difference in Types 1, 2 and 4 PPI settings [Type 1 ($p=0.0125$, $F=2.955$), Type 2 ($p=0.0074$,

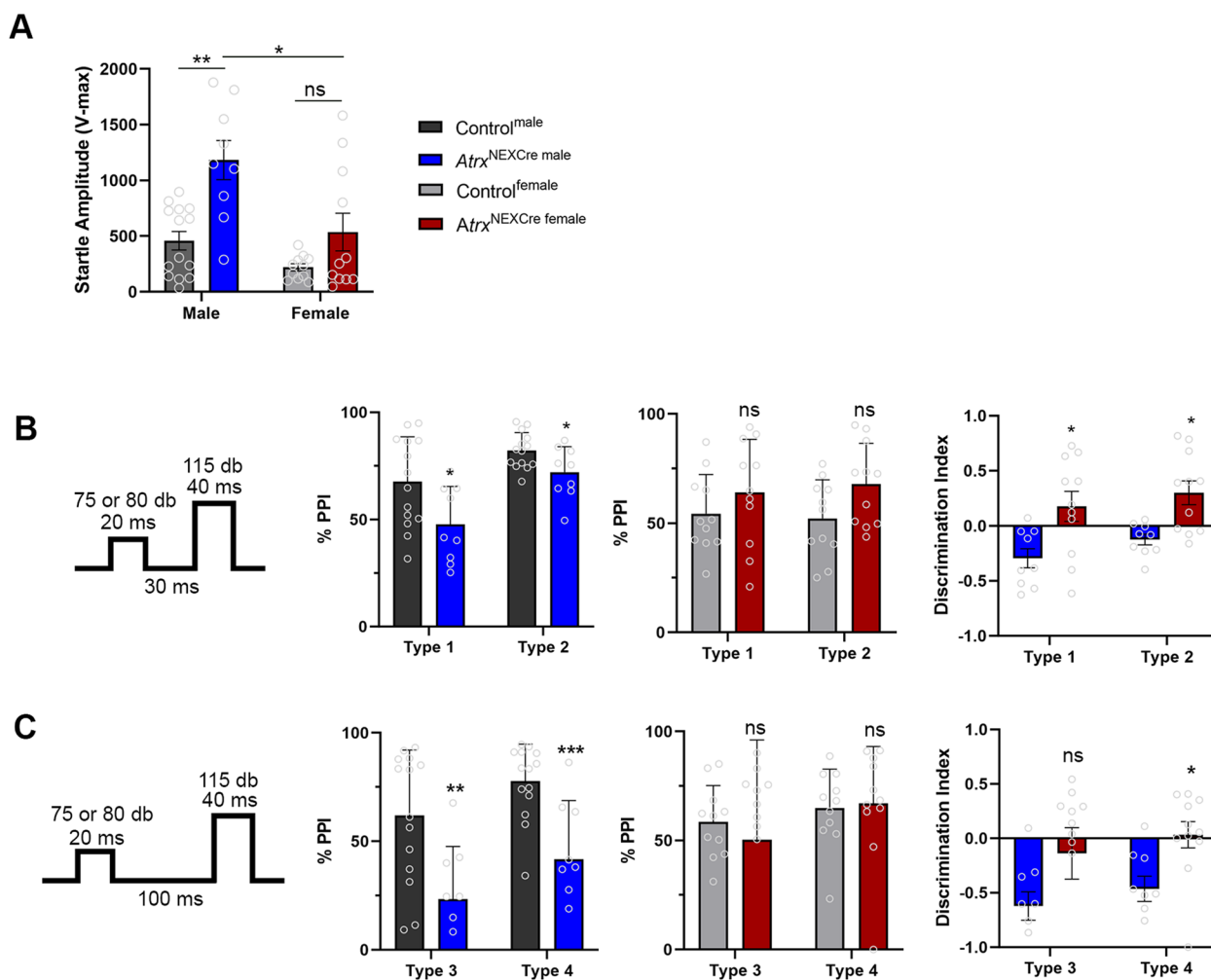


Fig. 4: *Atrx*^{NEXCre} mice exhibit sex-specific deficits in sensory gating. **A** *Atrx*^{NEXCre} male mice display an exaggerated auditory startle response compared to controls ($p=0.0008$, $F=18.08$), whereas *Atrx*^{NEXCre} females do not. **B** *Atrx*^{NEXCre} male mice exhibit decreased pre-pulse inhibition for Type 1 (30ms, 75db) ($p=0.0286$, $F=1.414$), Type 2 (30ms, 80db) ($p=0.0261$, $F=2.048$), **C** Type 3 (75db, 100ms) ($p=0.0042$, $F=1.549$) and Type 4 settings (80db, 100ms) ($p=0.0008$, $F=2.510$). Control^{male} $n=14$, *Atrx*^{NEXCre} male $n=9$, Control^{female} $n=11$, *Atrx*^{NEXCre} female $n=11$. Sex differences were detected in Type 1 ($p=0.0125$, $F=2.955$), Type 2 ($p=0.0074$, $F=6.064$), and Type 4 settings ($p=0.0093$, $F=1.338$). Error bars represent \pm -SEM. Students t-test, Mann Whitney, or Two-way Anova with Sidak post-hoc performed when appropriate (* $p<0.05$, ** $p<0.001$, *** $p<0.0001$)

F=6.064), and Type 4 ($p=0.0093$, F=1.338)]. Together these data reveal a male-specific effect of ATRX loss on sensory gating. In addition to auditory sensory gating, olfaction is another disrupted sensory process implicated in patients with ASD [38]. We found that loss of ATRX significantly affects olfaction in both male and female *Atrx*^{NEXCre} mice, indicating an additional sensory processing deficit in these mice (Fig. S3B).

Social behaviour deficits in *Atrx*^{NEXCre} mice

The three-chamber test was used to evaluate social phenotypes. All experimental animals freely explored the chamber during a 10-minute habituation period (Fig. S3B). Control and *Atrx*^{NEXCre} mice displayed the expected preference for the stranger mouse over the object in this test (Fig. 5A). Impaired social memory is commonly observed in patients with ASD. In mouse models, social memory can be assessed during the third

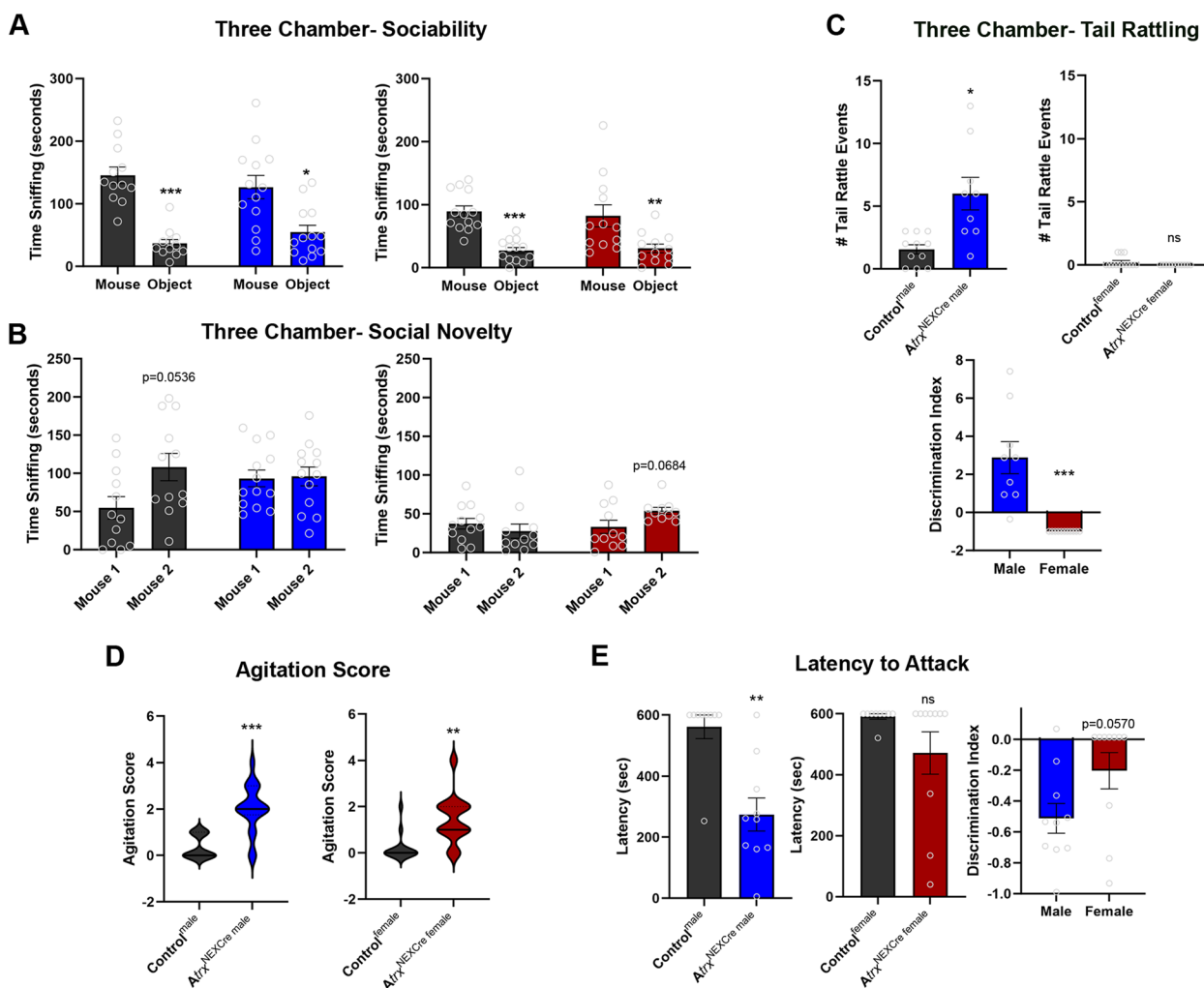


Fig. 5 Sex-specific altered social behaviour in *Atrx*^{NEXCre} mice. **A** Control and *Atrx*^{NEXCre} mice of both sexes spend more time sniffing the stranger mouse compared to the object in the three-chamber test (Control^{male} $p<0.0001$, *Atrx*^{NEXCre male} $p=0.0017$, Control^{female} $p<0.0001$, *Atrx*^{NEXCre female} $p=0.0005$). **B** Male *Atrx*^{NEXCre} mice show no preference for a novel mouse in the social novelty portion of the three-chamber test (Control^{male}: $n=12$, *Atrx*^{NEXCre male} $n=13$). This test yields inconclusive results for female mice, as the controls did not show a preference for the novel mouse (Control^{female}: $n=11$, *Atrx*^{NEXCre female} $n=12$). **C** *Atrx*^{NEXCre} male mice exhibit significantly more tail rattling events in the presence of a stranger mouse ($p=0.0013$, $F=10.35$), while *Atrx*^{NEXCre} female mice do not exhibit this behaviour. **D** *Atrx*^{NEXCre} male and female mice are more agitated upon handling, as determined by an elevated agitation score (Male: $p<0.0001$, $F=4.160$, Control^{male} $n=11$, *Atrx*^{NEXCre male} $n=18$, Female: $p=0.0003$, $F=3.290$, Control^{female} $n=14$, *Atrx*^{NEXCre female} $n=13$). **E** *Atrx*^{NEXCre} male mice exhibit decreased latency to attack in the juvenile resident intruder paradigm, and *Atrx*^{NEXCre} female mice do not (Male: $p=0.0006$, $F=2.187$, Control^{male} $n=9$, *Atrx*^{NEXCre male} $n=10$, Female: Control^{female} $n=9$, *Atrx*^{NEXCre female} $n=10$). Error bars represent +/-SEM. Two-way Anova with Sidak post-hoc, Students t-test, or Mann Whitney performed when appropriate (* $p<0.05$, ** $p<0.001$, *** $p<0.0001$).

part of the three-chamber test, which involves a social novelty test. As expected, control male mice spent more time with the novel mouse, although this did not reach the significance criteria ($p=0.0536$), while *Atrx*^{NEXCre} male mice did not. This indicates that the *Atrx*^{NEXCre} male mice may have a social memory deficit (Fig. 5B). The social memory test performed with female mice was inconclusive as the control mice failed show a preference for the novel mouse in this paradigm (Fig. 5B).

We noticed that *Atrx*^{NEXCre} males were exhibiting a tail rattling phenotype when in the presence of the stranger mice during the three-chamber test. Tail rattling is typically identified as an aggressive behaviour in mice, often associated with fear or to show threat in aggressive social encounters [39]. Quantification shows that *Atrx*^{NEXCre} male mice exhibit significantly more tail rattling events at the stranger mouse compared to controls ($p=0.0013$, $F=10.35$) and that female mice do not exhibit this behaviour (Fig. 5C). These results identify a male-specific increase in social aggression in *Atrx*^{NEXCre} mice. Additionally, we observed that *Atrx*^{NEXCre} mice are agitated in the presence of a handler. We quantified this unusual behaviour using an agitation score (0-5) that reflects biting, trunk curl and vocalization events during handling (Movie 2). According to these criteria, both *Atrx*^{NEXCre} male and female mice are significantly more agitated upon handling compared to controls (Male: $p<0.0001$, $F=4.160$, Female: $p=0.0003$, $F=3.290$) (Fig. 5D). No sex differences were identified for the agitation score. We also found that *Atrx*^{NEXCre} male mice were aggressive towards their littermates, occasionally resulting in separation due to injuries (8/35 cages). Issues with littermates fighting was not noted with *Atrx*^{NEXCre} female mice. To establish the extent of this aggressive behaviour, we performed a juvenile resident intruder assay. The results show that *Atrx*^{NEXCre} male mice have a decreased latency of attack, showing a significant increase in aggression not seen with *Atrx*^{NEXCre} female mice (Male: $p=0.0006$, $F=2.187$) (Fig. 5E). The discrimination index indicates no significant sex difference in their response to the intruder (Fig. 5E).

Discussion

The main goal of this study was to determine if embryonic deletion of ATRX in forebrain excitatory neurons would result in a broader spectrum of deficits than previously observed when ATRX is deleted postnatally in these same neurons. When ATRX is deleted postnatally in excitatory neurons, the mice display impaired long term spatial memory without ASD-like features [27, 28]. However, ATR-X syndrome patients exhibit more widespread cognitive and neurological problems [15]. Therefore, we hypothesized that earlier deletion of *Atrx* was

required to induce ASD-associated traits. Indeed, we identified the two core ASD features in adult *Atrx*^{NEXCre} mice: social deficits and repetitive behaviours. We also observed hyperactivity and a male-specific deficit in acoustic sensory gating. According to the DSM-V [40], impaired sensory processing is now considered a core feature of ASD. Based on the published and current models of ATRX inactivation in neurons, there could be a period of vulnerability (mid-gestation to early adolescence) where the dorsal forebrain is highly sensitive to ATRX loss of function, with dire consequences on behaviour in adulthood, particularly for autistic-like traits. This is supported by previous reports showing that ASD risk genes are expressed at high levels in the cortex in mid-to-late fetal development and largely enriched in maturing excitatory neuron lineages [41]. In addition, studies show that patients with ASD have atypical brain development, with changes in proper neuronal migration in the cortex [42] and many transcription factors that appear in mid-gestation and play an important role in corticogenesis have been shown to be ASD-risk genes [43, 44].

The *Atrx*^{NEXCre} mice characterized in this study offer a good model to help understand the structural and molecular changes that occur early during forebrain development and lead to altered cognitive abilities. Research focusing on mouse models with mutations in synaptic proteins have found similar behavioural alterations to the *Atrx*^{NEXCre} mice. For examples, mice with mutations in *Shank3*, a gene encoding a postsynaptic protein, exhibit hyper-reactive behaviours, increase in escape tendencies, aggression, and repetitive behaviours [45, 46]. Animal models containing mutations in the autistic linked post-synaptic neuroligin family of proteins display hyperactivity, repetitive behaviours and aggression [47–49]. Previously, our lab identified several ATRX target genes related to synaptic function, including *Neuroligin 4* (*Nlgn4*) that functions at the post-synaptic cleft and is a known autism-associated gene [50, 51]. Other relevant ATRX-regulated genes include miRNA137, whose target genes are involved in proper synapse function [27] and *Xlr3b*, an imprinted gene involved in the regulation of mRNA transport in dendrites [52]. Future work should focus on characterizing the transcriptional changes in the male and female *Atrx*^{NEXCre} mice during the identified period of vulnerability to gain mechanistic understanding of the ensuing cognitive dysfunction.

We observed significant deficits in fear memory in *Atrx*^{NEXCre} mice of both sexes. This contrasts with *Atrx*^{CamKII α Cre} mice (deletion starting at ~P20), in which fear memory deficits were only observed in males [27]. Female protection theories have been extensively reviewed and suggest that estrogen levels play a neuroprotective role in preventing cognitive impairments [53, 54]. A previous

study used a computational model to investigate molecular networks of copy number variants (CNVs) in both male and female patients with ASD. They found that CNVs in females affect a larger number of genes, and that genes disrupted in female ASD patients were functionally more important in molecular networks. These data support previous hypotheses suggesting that females need to experience a harsher effect on connectivity than males to experience ASD symptoms [55]. The difference in this protective effect between the *Atrx*^{CamKIIICre} and *Atrx*^{NEX-Cre} female mice suggests that in a neuroplastic setting, hormones can impart neuroprotective effect; however, in the case of an embryonic deletion, the anomalous network connectivity might not be as malleable. Investigation into the sex-specific cellular and connectivity changes in *Atrx*^{NEXCre} mice could shed light on protective mechanisms or reversibility of the observed behaviours.

In our model, both male and female *Atrx*^{NEXCre} mice exhibit hyperactivity, repetitive behaviours, and olfactory deficits. We also identified additional male-specific behaviour changes, including social aggression, social memory deficits, acoustic hypersensitivity and decreased PPI. Clinically, males are biased in diagnosis of many neurodevelopmental disorders, including ID, ASD, and ADHD. The reason, whether female protection, male vulnerability, diagnosis bias, or societal differences between males and females is highly debated [56, 57]. Within the scientific literature, there is an increasing concern regarding the under identification of ASD in females when compared to males [58]. Presently, there is a dearth of comprehensive research that encompasses both male and female mice in their investigations. Consequently, it is unclear how females are affected compared to males, impeding our understanding of the underlying reasons for underdiagnosis. Acquisition of sex-specific data in ASD could prove instrumental in elucidating this phenomenon.

Conclusions

The behavioural characterization of the *Atrx*^{NEXCre} mouse model establishes it as a viable system for studying a range of neurological abnormalities associated with ATRX dysfunction. This model holds potential in unravelling the mechanisms related to the vulnerable period for ASD during brain development, as well as shedding light

on sex differences in ASD and theories of female protection. More work is required to identify potential connectivity disruptions, downstream targets affected by ATRX loss, and the overall molecular and structural distinctions between male and female *Atrx*^{NEXCre} mice. Ultimately, this model provides a clinically relevant platform to identify therapeutic targets and serves as a preclinical model for testing potential therapies.

Materials and methods

Animal care and husbandry

All experiments were performed using *Mus musculus*, generated with conditional inactivation of *Atrx* in post-mitotic excitatory neurons starting at E11.5, by crossing 129SV female mice heterozygous for *Atrx*^{loxP} sites [24] with C57BL/6 male mice expressing Cre recombinase under the control of NEX-Cre gene promoter (Neurod6^{tm1(cre)Kan}) [29]. Male progeny with a floxed *Atrx* allele on the X chromosome and the transgenic NEXCre allele are ATRX-null (*Atrx*^{NEXCre male}). Control male and female mice only have the NEXCre allele (Control^{male}, Control^{female}). To obtain homozygous *Atrx*^{loxP} females, 129SV female mice heterozygous for *Atrx*^{loxP} sites are crossed with C57BL/6;129SV male mice expressing NEX-Cre and have a floxed *Atrx* allele, offspring homozygous for *Atrx*^{loxP} expressing NEXCre are knockouts (*Atrx*^{NEXCre female}). Mice were exposed to a 12-hour-light/12-hour-dark cycle with water and chow ad libitum. All procedures involving animals were conducted in accordance with the regulations of the Animals for Research Act of the province of Ontario and approved by the University of Western Ontario Animal Care and Use Committee (2021-049). Ear notch biopsies were taken at P8-10 for animal ID and genotyping purposes. Genotyping was performed as previously described [24] using the primers in Table 1.

Immunofluorescence and microscopy

For histological analysis of embryonic samples, timed matings were arranged late afternoon and the following midday, day of vaginal plug discovery, was considered embryonic day (E)0.5. At E13.5 pregnant females were anesthetized by CO₂, sacrificed by cervical dislocation, and embryos were dissected and placed into 4% PFA overnight for fixation. For histological analysis at

Table 1 Genotyping Primers

Allele	Forward Primer	Reverse Primer	Amplicon Size
<i>Atrx</i> WT	AGAAATTGAGGATGCTTCACC	TGAACCTGGGGACTTCTTTG	988bp
<i>Atrx</i> ^{loxP}	AGAAATTGAGGATGCTTCACC	CCACCATGATATTCGGCAAG	~1.2kb
NEXCre	TGACCAGAGTCATCCTTAGCG	AATGCTTCTGTCCGTTTGCC	~750bp

P20, mice were perfused with cold 1xPBS, followed by perfusion with cold 4% PFA overnight. After fixation all samples were washed with PBS and put into 30% sucrose for a minimum of one week prior to embedding in Cryomatrix™ (Epredia cat#6769006) in an 'ethanol-dry ice slurry,' and then placed at -80°C for storage. Samples were sectioned at 10µM thickness using a Leica cryostat (CM3050 S). Immunostaining was performed by rehydration in 1xPBS followed by an antigen retrieval by boiling in sodium citrate pH 6 containing 0.5% tween for 15 minutes. A permeabilization step consisting of a 10 min wash with 1xPBS containing 0.03% Triton X was followed by 1-hour of blocking in 1xPBS, 0.3% Triton X, 5% Goat serum. Primary antibodies were added in blocking solution [ATRX (Santa Cruz sc15408): 1:150 (Rb), βIII-tubulin (Biolegend 801201) 1:2000 (Ms), NeuN (Millipore MAB377): 1:150 (ms), PV (Sigma P3088): 1:1000 (Ms)] overnight at 4°C, followed by washing with 1xPBS, 0.3% Triton X solution. Secondary antibodies were added as appropriate (Thermo Scientific 1:1000 Alexa Fluor 488 anti-mouse cat#A11017, Alexa Fluor 594 anti-mouse cat#A11032, Alexa Fluor 594 anti-rabbit cat#A11012, Alexa Fluor 488 anti-rabbit cat#A11034) for 1 hour, slides washed with 1xPBS 0.3% Triton X, treated with a DAPI stain, washed, and mounted using ImmunoMount (Thermo Scientific cat# 9990402). Stained cryosections were imaged on a Leica microscope (CTR 6500) using Open-lab and Velocity version 6.0.1 software for analysis.

Behaviour Testing

Behavioral assessments were performed at 3-6 months of age, starting with less demanding tasks (open field tests, light-dark paradigm) to more demanding ones (contextual fear, resident intruder). ARRIVE guidelines were followed: animal groups were randomized, experimenters were blind to the genotypes, software-based analysis was used to score performance in all possible tasks. When software-based analysis was not possible, video recordings were coded and revealed to the experimenter after analysis. We have found that sample sizes of 10-15 per genotype is large enough to reach statistical significance in behavioural paradigms [27, 28, 59]. All behavioral experiments were performed between 9:00 AM and 4:00 PM.

Open-Field

Mice were placed in a 20 cm x 20 cm open arena with 30 cm high walls and left to explore for 1 hour. Animals were brought into the testing room 30 minutes prior to the start of the test to habituate to the room in their home cages. Locomotor activity, velocity, and distance travelled in the center of the open-field were all recorded in 5-minute intervals by AccuScan Instrument [59, 60].

Light/Dark Box

Mice were placed in a 40 cm x 40 cm arena with 30 cm high walls, and half the arena had a dark-box insert with a small open-slot where they could freely move back and forth between the light and dark areas. Animals were brought into the testing room in their home cages 15 minutes prior to the start of the test for habituation. Animals were placed in the light area of the apparatus and left to freely explore for 15-minutes. Time spent in the light-zone and dark-zone was measured in 5-minute intervals by AccuScan Instrument [60].

Grooming

Animals were individually habituated in an empty cage (home cage with no bedding) for 15 minutes prior to the start of the test. Mice were then recorded for 15 minutes using the Anymaze video-tracking system. The time spent grooming was manually scored from the videos [61].

Olfaction

The odor habituation and discrimination assay was performed as previously described [62]. Briefly, animals were habituated in a clean cage with a wire lid for 30 minutes prior to the start of the test. Mice were then presented with a cotton swab with either water, almond or banana flavouring (1:100 dilution of Club House extract). Each scent was presented for three sequential 2-minute trials and the time spent sniffing the odour was recorded. Sniffing was defined as the animal's nose oriented towards and near the cotton swab (2 cm or closer).

Three-Chamber

The three-chamber apparatus was used to observe sociability, as previously described [47] with minor modifications. Animals were habituated to the room for 20 minutes prior to beginning the assessment, and then allowed a 10-minute habituation trial where they freely explored the three-chamber apparatus containing wire cages to be used in the test trial. For the sociability test trial, on one side of the three-chamber a same-sex and age-matched wild-type C57Bl/6 stranger mouse was placed under the wire cage, and on the opposite side an object was placed under an identical wire cage. The test animal was then allowed to once again freely explore the apparatus. Time spent in each chamber was recorded by AnyMaze video-tracking system. The time spent sniffing the object and the mouse were scored from the videos. In the third portion of the test, the object was replaced with a novel mouse (mouse 2), and time spent sniffing mouse 1 and mouse 2 were recorded. Tail rattling events were obtained from the same videos [60]. To counterbalance any preference for one chamber over another, mouse 1

position was evenly distributed between the right or left chamber for both genotypes.

PPI

To assess sensory gating, we performed a startle response and pre-pulse inhibition test, as previously described [28, 37] (SR-LAB, San Diego Instruments). Briefly, animals were placed in the chamber apparatus and exposed to background noise (65 db) for 5-minutes for two habituation days prior to the test day. On test day, animals were again placed in the chamber and underwent a 10-minute acclimation with background noise (65 db), followed by a habituation block, which consisted of fifty acoustic startle pulses (115 db, 20 ms in length) at 20 second intervals. Finally, animals were exposed to a pre-pulse inhibition block which consisted of ten sets of five trial types randomly ordered with variable intervals of 10, 15 or 20 seconds between each trial. Four of the five trial types had a pre-pulse (75 or 80 db, 20 ms in length) 30 ms or 100 ms prior to the startle stimulus (115 db, 40 ms in length). The fifth trial type was the acoustic startle stimulus alone (115 db, 40 ms in length). The startle response represents the movement the platform, generating a measurable force by the SR-LAB software. The average startle response of the ten trials for trial type was calculated, and pre-pulse startle responses were normalized to the startle alone trial.

Fear memory

Fear memory was measured utilizing a 20 cm x 10 cm acrylic enclosure, as previously described [27] with minor modifications. The enclosure was wrapped in white paper, with a distinct striped wall on one side, a large black star on the opposite wall, and a metal grid floor. The metal grid floor was equipped with an electric shock generator, and a video recording was taken from above the apparatus and recorded using AnyMaze video tracking software. During the conditioning portion of the test, animals could freely explore the enclosure for 3-minutes. At the 150 second mark the animals were given a shock (2 mA, 180 V, ~1 second in length) through the metal grated floor and left to explore the cage another 30 seconds before returning to their home cage. Either 1.5 or 24-hours after receiving the shock, animals were placed back into the enclosure for 6-minutes and time spent freezing was measured. Time spent freezing is defined as complete immobility.

Morris Water Maze

The Morris water maze task was performed to determine alterations in spatial learning in memory, as previously described [27, 33] with minor modifications. The maze is a 1.5 m diameter pool with a water temperature of 26°C,

and black and white shapes act as spatial cues on each of the four walls surrounding the pool, creating four quadrants. During training, animals underwent four trials (90 s) a day for four consecutive days, with a 15-minute inter-trial period, to find a submerged platform (1.5 cm below the water surface). When mice failed to find the platform within the 90-second trial, they were gently guided to the platform and 90 seconds was recorded for that trial. All training trials were recorded, and movement monitored using AnyMaze tracking software.

Forced Swim Test

To test if mice displayed apathy in water, the forced swim test was performed [34]. Briefly, animals were placed in a beaker (15 cm diameter) of water (26°C, depth of 9 cm) for six-minutes. The first two minutes of the test was a habituation period, a camera positioned above the beaker recorded the last four-minutes of the test in AnyMaze software. Time spent immobile was determined during the four-minute test period. Time immobile refers to time floating with no tail or paw movement in the water. Small movements required to keep afloat was considered as time immobile.

Agitation score

We developed an agitation score based on handling during low-stress conditions. Three separate factors were combined to make a score from 0-5. First, a biting score was given (0-3) based on the number of times the handler was bitten (while wearing a protective glove) on three different days. Next, a 15-second video was taken moving the animal from one housing cage to another, and during the transfer the animal has held by the base of the tail for ~8 seconds. A trunk curl score (0=absent, 1=present) during 8 seconds of being held by the tail, and vocalization (0=absent, 1=present) during the 15 second video were also added for the total agitation score.

Resident Intruder

To assess aggression a resident-intruder paradigm was used, as previously described [47] with minor alterations. Experimental animals were separated and housed individually for 21 days prior to test day. Juvenile (8-10weeks of age) same-sex group-housed mice were used as intruders and were ~30-35% smaller in weight than experimental animals. Each intruder was only used once to avoid winner or loser effects. Intruders were introduced into the resident cage (at least a couple days dirty) and video tracking using AnyMaze software was recorded from above the resident cage. Testing ended after the first attack (defined as a bite) to prevent injury. If no attack occurred, the test ended at 10-minutes. The latency to attack was recorded as an indicator of aggression.

Statistical Analysis

All statistical analyses were performed using GraphPad Prism 9. For comparison of control to *Atrx*^{NEXCre} mice, a Students t-test was performed on time spent freezing for conditional fear memory; total distance travelled, average velocity, and distance travelled in center for the open field test; time spent in dark zone for the light/dark box paradigm; time spent grooming; %PPI; sociability index and number of tail rattling events for three-chamber test; agitation score; and latency to attack in the resident intruder paradigm. When variance was significant between samples, according to the F-statistic, a non-parametric Mann Whitney was performed. A two-way ANOVA was performed for distance over time analysis in the open field test, startle amplitude in the first portion of the PPI assessment, and for social preference in the three-chamber test. To evaluate sex differences, a discrimination index was calculated as follows: (*Atrx*^{NEXCre} value - average value for controls)/average value for controls. Discrimination indices for male and female mice were subjected to a Students t-test.

Abbreviations

ID	Intellectual disability
ASD	Autism spectrum disorder
ATRX	Alpha-thalassemia mental retardation, X-linked
cKO	conditional knockout
CNV	copy number variant

Supplementary Information

The online version contains supplementary material available at <https://doi.org/10.1186/s11689-023-09508-7>.

Additional file 1: Fig. S1. Validation of ATRX deletion in *Atrx*^{NEXCre} female mice. A) ATRX immunofluorescence staining (red) of E13.5 control and *Atrx*^{NEXCre} brain coronal cryosections. DAPI counterstaining is shown in blue. Scale bar, 570 μ m. B) Magnified view of ATRX (top, red) and β -tubulin (bottom, green) staining in the developing cortical plate. Scale bar, 144 μ m. C) ATRX (red) and DAPI (blue) staining in the cortex and hippocampus of *Atrx*^{NEXCre} and control mice at P20. D) ATRX (red) and NeuN (green) staining in the cortex and hippocampus at P20. Cortex scale bar, 100 μ m and hippocampus scale bar, 400 μ m. CA: cornu Ammonis, CP: cortical plate, Ctx: cortex, DG: dentate gyrus, GE: ganglionic eminence, LV: lateral ventricle, VZ: ventricular zone. eminence. Magnified images of cortical plate scale bar, 144 μ m. VZ: ventricular zone, CP: cortical plate. **Fig. S2.** Spatial learning deficits in *Atrx*^{NEXCre} mice. A) Latency to find the platform during the training phase of the Morris water maze test shows that *Atrx*^{NEXCre} male and female mice have impaired spatial learning ($p < 0.0001$, $F = 3.630$). B) *Atrx*^{NEXCre} mice spend less time swimming during the trials, reflecting their floating behaviour ($p < 0.0001$, $F = 19.50$) (Control^{male} $n = 7$, *Atrx*^{NEXCre} male $n = 7$, Control^{female} $n = 7$, *Atrx*^{NEXCre} female $n = 7$). C) A 6-minute forced swim test revealed increased apathy in water for male mice ($p = 0.0292$, $F = 2.028$) (Control^{male} $n = 15$, *Atrx*^{NEXCre} male $n = 12$) and decreased apathy in female mice ($p = 0.0154$, $F = 3.149$, Control^{female} $n = 13$, *Atrx*^{NEXCre} female $n = 12$). Sex discrimination index reveals sex differences in the forced swim test ($p = 0.0002$, $F = 2.370$). Error bars represent \pm -SEM. Three-way ANOVA or Students t-test performed when appropriate (* $p < 0.05$, ** $p < 0.001$, *** $p < 0.0001$). **Fig. S3.** Self injury and reduced olfaction in *Atrx*^{NEXCre} mice. A) Example images of mice with evidence of self-injury caused by over-grooming. B) Male and female *Atrx*^{NEXCre} mice spend less time sniffing the almond and banana odors during the olfaction test ($p < 0.0001$,

$F = 18.65$; Control^{male} $n = 17$, *Atrx*^{NEXCre} male $n = 14$, Control^{female} $n = 13$, *Atrx*^{NEXCre} female $n = 13$). C) Male and female mice of each genotype explored the three-chamber apparatus freely during the 10-minute habituation portion of the three-chamber assay (Control^{male}: $n = 13$, *Atrx*^{NEXCre} male $n = 13$, Control^{female}: $n = 13$, *Atrx*^{NEXCre} female $n = 11$) (L= left side, C= center, R= right side). Error bars represent \pm -SEM. Two-way Anova with Sidak post-hoc (* $p < 0.05$, ** $p < 0.001$, *** $p < 0.0001$).

Additional file 2.

Additional file 3.

Additional file 4.

Additional file 5.

Acknowledgments

We are grateful for access to the Neurobehavioural Core Facility at the Roberts Research Institute and for the support of facility manager Matthew Cowan.

Authors' contributions

K.M.Q. contributed to conceptualization, design and execution of experiments, data interpretation, and writing of article. N.M.K. contributed to execution of experiments and data interpretation. N.G.B. contributed the conception, design, interpretation of data, and writing of article.

Funding

K.Q. was the recipient of an Ontario Graduate Scholarship, a graduate studentship from the Department of Paediatrics at Western University, and the Sir Fredrick Banting CIHR Doctoral Award. N.M.K. received a graduate studentship from the Department of Paediatrics at Western University. This work was supported by BrainsCAN through the Canada First Research Excellence Fund and by operating funds from the Canadian Institutes for Health Research to NGB (MOP142369).

Availability of data and materials

All data generated or analyzed during this study are included in this published article.

Declarations

Ethics approval and consent to participate

Not applicable.

Consent for publication

Not applicable.

Competing interests

No competing interests declared.

Received: 4 August 2023 Accepted: 1 November 2023

Published online: 13 November 2023

References

- Fahrner JA, Bjornsson HT. Mendelian disorders of the epigenetic machinery: tipping the balance of chromatin states. *Annu Rev Genomics Hum Genet.* 2014;15:269–93.
- Maulik PK, Mascarenhas MN, Mathers CD, Dua T, Saxena S. Prevalence of intellectual disability: A meta-analysis of population-based studies. *Res Dev Disabil.* 2011;
- Bougeard C, Picarel-Blanchot F, Schmid R, Campbell R, Buitelaar J. Prevalence of Autism Spectrum Disorder and Co-morbidities in Children and Adolescents: A Systematic Literature Review. *Front Psychiatry.* 2021;
- Abrahams BS, Geschwind DH. Advances in autism genetics: on the threshold of a new neurobiology. *Nat Rev Genet.* 2008;9:341–55.
- Baio J, Wiggins L, Christensen D, et al. Prevalence of Autism Spectrum Disorder Among Children Aged 8 years- Autism and Developmental Disabilities Monitoring Network. *MMWR Surveill Summ.* 2014;67:1–23.

6. Fitzpatrick SE, Srivorakiat L, Wink LK, Pedapati EV, Erickson CA. Aggression in autism spectrum disorder: presentation and treatment options. *Neuropsychiatr Dis Treat*. 2016;12:1525–38.
7. Kas MJ, Glennon JC, Buitelaar J, Ey E, Biemans B, Crawley J, et al. Assessing behavioural and cognitive domains of autism spectrum disorders in rodents: current status and future perspectives. *Psychopharmacol (Berl)*. 2014;231:1125–46. <https://doi.org/10.1007/s00213-013-3268-5>.
8. Barrett RM, Malvaez M, Kramar E, Matheos DP, Arrizon A, Cabrera SM, et al. Hippocampal focal knockout of CBP affects specific histone modifications, long-term potentiation, and long-term memory. *Neuropsychopharmacology*. 2011;36:1545–56.
9. Feng J, Zhou Y, Campbell SL, Le T, Li E, Sweatt JD, et al. Dnmt1 and Dnmt3a maintain DNA methylation and regulate synaptic function in adult forebrain neurons. *Nat Neurosci*. 2010;13:423–30.
10. Levenson JM, Roth TL, Lubin FD, Miller CA, Huang I-C, Desai P, et al. Evidence that DNA (cytosine-5) methyltransferase regulates synaptic plasticity in the hippocampus. *J Biol Chem*. 2006;281:15763–73.
11. Kochinke K, Zweier C, Nijhof B, Fenckova M, Cizek P, Honti F, et al. Systematic Phenomics Analysis Deconvolutes Genes Mutated in Intellectual Disability into Biologically Coherent Modules. *Am J Hum Genet*. 2016;98:149–64.
12. Gibbons RJ, Wada T, Fisher CA, Malik N, Mitson MJ, Steensma DP, et al. Mutations in the chromatin-associated protein ATRX. *Hum Mutat*. 2008;29:796–802.
13. Garrick D, Samara V, McDowell TL, Smith AJH, Dobbie L, Higgs DR, et al. A conserved truncated isoform of the ATR-X syndrome protein lacking the SWI/SNF-homology domain. *Gene*. 2004;326:23–34.
14. Gibbons RJ, Picketts DJ, Villard L, Higgs DR. Mutations in a putative global transcriptional regulator cause X-linked mental retardation with alpha-thalassemia (ATR-X syndrome). *Cell*. 1995;80:837–45.
15. Gibbons RJ, Higgs DR. Molecular-clinical spectrum of the ATR-X syndrome. *Am J Med Genet*. 2000;97:204–12.
16. Grozeva D, Carss K, Spasic-Boskovic O, Tejada M-I, Gecz J, Shaw M, et al. Targeted Next-Generation Sequencing Analysis of 1,000 Individuals with Intellectual Disability. *Hum Mutat*. 2015;36:1197–204.
17. Gong X, Bacchelli E, Blasi F, Toma C, Betancur C, Chaste P, et al. Analysis of X chromosome inactivation in autism spectrum disorders. *Am J Med Genet B Neuropsychiatr Genet*. 2008;147B:830–5.
18. Li J, Wang L, Guo H, Shi L, Zhang K, Tang M, et al. Targeted sequencing and functional analysis reveal brain-size-related genes and their networks in autism spectrum disorders. *Mol Psychiatry*. 2017;22:1282–90.
19. Bérubé NG, Smeenk CA, Picketts DJ. Cell cycle-dependent phosphorylation of the ATRX protein correlates with changes in nuclear matrix and chromatin association. *Hum Mol Genet*. 2000;9:539–47.
20. Law MJ, Lower KM, Voon HPJ, Hughes JR, Garrick D, Viprakasit V, et al. ATR-X syndrome protein targets tandem repeats and influences allele-specific expression in a size-dependent manner. *Cell*. 2010;143:367–78.
21. Meyer-Nava S, Torres A, Zurita M, Valadez-Graham V. Molecular effects of dADD1 misexpression in chromatin organization and transcription. *BMC Mol Cell Biol*. 2020;21:17.
22. Wong LH, McGhie JD, Sim M, Anderson MA, Ahn S, Hannan RD, et al. ATRX interacts with H3.3 in maintaining telomere structural integrity in pluripotent embryonic stem cells. *Genome Res*. 2010;20:351–60.
23. Garrick D, Sharpe JA, Arkell R, Dobbie L, Smith AJH, Wood WG, et al. Loss of Atrx affects trophoblast development and the pattern of X-inactivation in extraembryonic tissues. *PLoS Genet*. 2006;2:e58.
24. Berube NG, Mangelsdorf M, Jagla M, Vanderluit J, Garrick D, Gibbons RJ, et al. The chromatin-remodeling protein ATRX is critical for neuronal survival during corticogenesis. *J Clin Invest*. 2005;115:258–67.
25. Seah C, Levy MA, Jiang Y, Mokhtarzada S, Higgs DR, Gibbons RJ, et al. Neuronal death resulting from targeted disruption of the Snf2 protein ATRX is mediated by p53. *J Neurosci*. 2008;28:12570–80.
26. Watson LA, Solomon LA, Li JR, Jiang Y, Edwards M, Shin-ya K, et al. Atrx deficiency induces telomere dysfunction, endocrine defects, and reduced life span. *J Clin Invest*. 2013;123:2049–63.
27. Tamming RJ, Dumeaux V, Jiang Y, Shafiq S, Langlois L, Ellegood J, et al. Atrx Deletion in Neurons Leads to Sexually Dimorphic Dysregulation of miR-137 and Spatial Learning and Memory Deficits. *Cell Rep*. 2020;31:107838.
28. Martin-Kenny N, Bérubé NG. Effects of a postnatal Atrx conditional knockout in neurons on autism-like behaviours in male and female mice. *J Neurodev Disord*. 2020;12:17. <https://doi.org/10.1186/s11689-020-09319-0>.
29. Goebbels S, Bormuth I, Bode U, Hermanson O, Schwab MH, Nave K-A. Genetic targeting of principal neurons in neocortex and hippocampus of NEX-Cre mice. *Genesis*. 2006;44:611–21.
30. Ross SE, Greenberg ME, Stiles CD. Basic helix-loop-helix factors in cortical development. *Neuron*. 2003;39:13–25.
31. Dieni C, Chancey J, Overstreet-Wadiche L. Dynamic functions of GABA signaling during granule cell maturation. *Front Neural Circuits*. 2013;113. <https://doi.org/10.3389/fncir.2012.00113>.
32. Mamiya N, Fukushima H, Suzuki A, Matsuyama Z, Homma S, Frankland PW, et al. Brain Region-Specific Gene Expression Activation Required for Reconsolidation and Extinction of Contextual Fear Memory. *J Neurosci*. 2009;29:402. Available from: <http://www.jneurosci.org/content/29/2/402.abstract>
33. Vorhees C, v, Williams MT. Morris water maze: procedures for assessing spatial and related forms of learning and memory. *Nat Protoc*. 2006;1:848–58.
34. Can A, Dao DT, Arad M, Terrillon CE, Piantadosi SC, Gould TD. The Mouse Forced Swim Test. *J Visual Experim*. 2011;
35. Simonoff E, Pickles A, Charman T, Chandler S, Loucas T, Baird G. Psychiatric disorders in children with autism spectrum disorders: Prevalence, comorbidity, and associated factors in a population-derived sample. *J Am Acad Child Adolesc Psychiatry*. 2008;47
36. Luo J, Norris RH, Gordon SL, Nithianantharajah J. Neurodevelopmental synaptopathies: Insights from behaviour in rodent models of synapse gene mutations. *Prog Neuropsychopharmacol Biol Psychiatry*. Elsevier Inc; 2018. p. 424–39.
37. Davis M. The Mammalian Startle Response. *Neural Mechan Startle Behav*. 1984;
38. Sweigert JR, St. John T, Begay KK, Davis GE, Munson J, Shankland E, et al. Characterizing olfactory function in children with autism spectrum disorder and children with sensory processing dysfunction. *Brain Sci*. 2020;10.
39. Scott JP. Agonistic behavior of mice and rats: A review. *Integr Comp Biol*. 1966;6
40. American Psychiatric Association. *Diagnostic and Statistical Manual of Mental Disorders*. American Psychiatric Association; 2013.
41. Satterstrom FK, Kosmicki JA, Wang J, Breen MS, De Rubeis S, An JY, et al. Large-Scale Exome Sequencing Study Implicates Both Developmental and Functional Changes in the Neurobiology of Autism. *Cell*. 2020;180
42. Hutsler JJ, Love T, Zhang H. Histological and Magnetic Resonance Imaging Assessment of Cortical Layering and Thickness in Autism Spectrum Disorders. *Biol Psychiatry*. 2007;61:449–57. Available from: <https://www.sciencedirect.com/science/article/pii/S0006322306001478>
43. Kwan KY. Transcriptional dysregulation of neocortical circuit assembly in ASD. *Int Rev Neurobiol*. 2013;
44. Fazel Darbandi S, Robinson Schwartz SE, Pai ELL, Everitt A, Turner ML, Cheyette BNR, et al. Enhancing WNT Signaling Restores Cortical Neuronal Spine Maturation and Synaptogenesis in Tbr1 Mutants. *Cell Rep*. 2020;31.
45. Drapeau E, Riad M, Kajiwara Y, Buxbaum JD. Behavioral Phenotyping of an Improved Mouse Model of Phelan-McDermid Syndrome with a Complete Deletion of the Shank3 Gene. *eNeuro*. 2018:5.
46. Zhang F, Rein B, Zhong P, Shwani T, Conrow-Graham M, Wang Z-J, et al. Synergistic inhibition of histone modifiers produces therapeutic effects in adult Shank3-deficient mice. *Transl Psychiatry*. 2021;11:99. <https://doi.org/10.1038/s41398-021-01233-w>.
47. El-Kordi A, Winkler D, Hammerschmidt K, Kästner A, Krueger D, Ronnenberg A, et al. Development of an autism severity score for mice using Nlgn4 null mutants as a construct-valid model of heritable monogenic autism. *Behav brain res*. 2013;251:41–9.
48. Rothwell PE, Fuccillo MV, Maxeiner S, Hayton SJ, Gokce O, Lim BK, et al. Autism-associated neuroligin-3 mutations commonly impair striatal circuits to boost repetitive behaviors. *Cell*. 2014;158:198–212. Available from: <https://www.ncbi.nlm.nih.gov/pubmed/24995986>
49. Kohl C, Wang X-D, Grosse J, Fournier C, Harbich D, Westerholz S, et al. Hippocampal neuroligin-2 links early-life stress with impaired social recognition and increased aggression in adult mice. *Psychoneuroendocrinol*. 2015;55:128–43.
50. Levy MA, Kernohan KD, Jiang Y, Berube NG. ATRX promotes gene expression by facilitating transcriptional elongation through guanine-rich coding regions. *Hum Mol Genet*. 2015;24:1824–35.

51. Jamain S, Quach H, Betancur C, Råstam M, Colineaux C, Gillberg C, et al. Mutations of the X-linked genes encoding neuroligins NLGN3 and NLGN4 are associated with autism. *Nat Genet.* 2003;34
52. Shioda N, Yabuki Y, Yamaguchi K, Onozato M, Li Y, Kurosawa K, et al. Targeting G-quadruplex DNA as cognitive function therapy for ATR-X syndrome. *Nat Med.* 2018;24:802–13. <https://doi.org/10.1038/s41591-018-0018-6>.
53. Azcoitia I, Barreto GE, Garcia-Segura LM. Molecular mechanisms and cellular events involved in the neuroprotective actions of estradiol. Analysis of sex differences. *Front Neuroendocrinol.* 2019;
54. Enriquez KD, Gupta AR, Hoffman EJ. Signaling Pathways and Sex Differential Processes in Autism Spectrum Disorder. *Front Psychiatry.* 2021;
55. Gilman SR, Iossifov I, Levy D, Ronemus M, Wigler M, Vitkup D. Rare De Novo Variants Associated with Autism Implicate a Large Functional Network of Genes Involved in Formation and Function of Synapses. *Neuron.* 2011;70
56. Rutherford M, McKenzie K, Johnson T, Catchpole C, O'Hare A, McClure I, et al. Gender ratio in a clinical population sample, age of diagnosis and duration of assessment in children and adults with autism spectrum disorder. *Autism.* 2016;20
57. Ferri SL, Abel T, Brodtkin ES. Sex Differences in Autism Spectrum Disorder: a Review. *Curr Psychiatry Rep.* 2018;20
58. Kilmer M, Boykin AA. Analysis of the 2000 to 2018 autism and developmental disabilities monitoring network surveillance reports: Implications for primary care clinicians. *J Pediatr Nurs.* 2022;65.
59. Tamming RJ, Siu JR, Jiang Y, Prado MAM, Beier F, Berube NG. Mosaic expression of Atrx in the mouse central nervous system causes memory deficits. *Dis Model Mech.* 2017;10:119–26.
60. Cogram P, Deacon RMJ, Warner-Schmidt JL, von Schimmelmann MJ, Abrahams BS, During MJ. Gaboxadol Normalizes Behavioral Abnormalities in a Mouse Model of Fragile X Syndrome. *Front Behav Neurosci.* 2019;141. <https://doi.org/10.3389/fnbeh.2019.00141>.
61. Stoodley CJ, D'Mello AM, Ellegood J, Jakkamsetti V, Liu P, Nebel MB, et al. Altered cerebellar connectivity in autism and cerebellar-mediated rescue of autism-related behaviors in mice. *Nat Neurosci.* 2017;20:1744–51. <https://doi.org/10.1038/s41593-017-0004-1>.
62. Arbuckle EP, Smith GD, Gomez MC, Lugo JN. Testing for Odor Discrimination and Habituation in Mice. *J Visual Experim.* 2015;

Publisher's Note

Springer Nature remains neutral with regard to jurisdictional claims in published maps and institutional affiliations.

Ready to submit your research? Choose BMC and benefit from:

- fast, convenient online submission
- thorough peer review by experienced researchers in your field
- rapid publication on acceptance
- support for research data, including large and complex data types
- gold Open Access which fosters wider collaboration and increased citations
- maximum visibility for your research: over 100M website views per year

At BMC, research is always in progress.

Learn more biomedcentral.com/submissions

